Biochemistry and Biophysics Reports 38 (2024) 101682

Contents lists available at ScienceDirect

Biochemistry and Biophysics Reports

journal homepage: www.elsevier.com/locate/bbrep

cFLIP – An interacting partner and a novel substrate for pro-apoptotic serine protease HtrA2

Kalyani Natu [a,b], Shubhankar Dutta [a,b], Kakoli Bose [a,b,*]

[a] Integrated Biophysics and Structural Biology Lab, Advanced Centre for Treatment Research and Education in Cancer (ACTREC), Tata Memorial Centre, Mumbai, 410210, India
[b] Homi Bhabha National Institute, BARC Training School Complex, Mumbai, 400094, India

ARTICLE INFO

Keywords:
cFLIP
HtrA2
Apoptosis
DISC
Ischemia
Cancer

ABSTRACT

Background: HtrA2, a pro-apoptotic protease, plays a crucial role in apoptosis by cleaving inhibitory and anti-apoptotic proteins by translocating from mitochondria to the cytosol. Prior studies in ischemic cells have indicated that cytosolic HtrA2 triggers cFLIP degradation, plausibly through direct interaction. In this study, we have characterized the cFLIP protein, validated its interaction with HtrA2, and demonstrated that cFLIP is also a substrate of HtrA2.
Methods: We have identified the probable cleavage sites of cFLIP through gel-based assays and mass spectrometric analysis of the cleaved fragments.
Results: Our findings shed light on a key protein-protein interaction involving pro-apoptotic HtrA2, confirming cFLIP as its interacting partner and substrate.
Conclusion: Understanding the nuances of HtrA2's interaction with cFLIP (a decoy protein of the initiator procaspase-8 in the extrinsic apoptotic pathway) and deciphering the cFLIP's mode of cleavage, would provide an excellent alternative to modulate the pathway for therapeutic benefits toward diseases like ischemia and cancer.

1. Introduction

Apoptosis is a genetically controlled process that maintains homeostasis [1]. HtrA2 is a highly conserved allosterically regulated [2], pro-apoptotic protein localized in the mitochondria that relocates to the cytosol upon apoptotic trigger [3,4]. In the cytosol, HtrA2 plays a key role in activating apoptotic pathways in both caspase-dependent and independent manner [5]. HtrA2's serine protease activity enables direct cleavage of specific death effector domain (DED) containing anti-apoptotic proteins like Pea15 thus promoting apoptosis. The domains of HtrA2 exhibit a trimeric pyramidal architecture where the IAP binding AVPS motif is at the apex (N terminus), the catalytic serine protease domain (SPD) at the centre (together with N-terminus is referred as N-SPD), while the PDZ (Postsynaptic density-95/Discs large/Zonula occludens-1) domain forms the base and controls access to the SPD by its substrates.

Evasion of apoptosis is a hallmark of cancer and a key mechanism of cancer cell resistance. This occurs mainly through the overexpression of antiapoptotic proteins one of which is Cellular FLICE Like Inhibitory Protein (cFLIP). cFLIP, a pseudo-protease, is a structural analogue of the zymogen of initiator caspase procaspase-8. cFLIP has the 'death–fold superfamily' motif for interaction, the tandem (DEDs) that play a key role in cell death. DEDs feature a globular structure with six amphipathic, anti-parallel α-helices, forming a conserved hydrophobic core upon folding [6]. Thus, cell fate relies on DED-containing proteins, vital regulators of cell survival and death. In ischemic heart cells, research suggests a possible interaction between two apoptotic pathway proteins, hypothesizing that HtrA2 may cleave cFLIP. However, these speculative observations lack direct evidence and hence a thorough investigation of these interactions especially with anti-apoptotic proteins like cFLIP, crucial for evading apoptosis become imperative.

Our study is the first to demonstrate the interaction between HtrA2 and cFLIP using purified human recombinant proteins and computational, biochemical, and biophysical analyses. Biophysical characterization determines the secondary structure, stability, and folding of cFLIP. Moreover, through multiple experiments we delineate the

* Corresponding author. Integrated Biophysics and Structural Biology Lab, Advanced Centre for Treatment Research and Education in Cancer (ACTREC), Tata Memorial Centre, Mumbai, 410210, India.
E-mail addresses: rkk8293@gmail.com (K. Natu), skdutta2091@gmail.com (S. Dutta), kbose@actrec.gov.in (K. Bose).

https://doi.org/10.1016/j.bbrep.2024.101682
Received 22 January 2024; Received in revised form 29 February 2024; Accepted 29 February 2024

interaction between HtrA2 and cFLIP at the domain level. Also, our study provides the first direct evidence that HtrA2 cleaves cFLIP through enzyme assays with purified proteins. Furthermore, we predict the plausible cleavage site(s) of HtrA2 on cFLIP through mass spectrometric analysis of the cleaved fragment(s). These findings offer insights into the interplay of proteins within apoptotic pathways, shedding light on how these pathways overlap at various stages to determine cell fate. Exploring such novel protein-protein interactions, here, cFLIP/HtrA2 deepen our understanding of pathways crucial for exploring their roles in complex diseases like cancer, neurodegeneration, and ischemic heart diseases facilitating the identification of new drug targets for therapeutic benefits. Further research aims to validate the exact binding and cleavage sites on cFLIP to provide more comprehensive understanding.

2. Materials and methods

2.1. Purification and biophysical characterization of full-length cFLIP

Full-length cFLIP was cloned **(Supplementary M1)** and purified using affinity chromatography on Ni-NTA resin. The buffer system comprised of 20 mM Na_2HPO_4 with 150 mM NaCl and 5% glycerol for protein stability. For imidazole removal, protein was dialyzed against a buffer comprising 20 mM Na_2HPO_4 and 100 mM NaCl. Subsequently, the protein was concentrated using a centricon concentrator with an appropriate membrane cut-off for biophysical experiments (**Supplementary M2**).

2.2. Molecular modelling and docking of HtrA2 and cFLIP

Three-dimensional (3D) structural information for full-length cFLIP was unavailable, hence, its predicted model was retrieved from AlphaFold database (AlphaFold ID: AF-O15519-F1) for *in-silico* docking and MD (Molecular Dynamics) simulation studies. In case of HtrA2, the active 3D structure (PDB ID: 5M3N) was retrieved from Protein Data Bank and the missing loop regions were remodelled prior to the generation of HtrA2 trimer [7]. Loop filling details are given in **Supplementary M3** For preliminary binding analysis, the HtrA2 trimer and cFLIP were subjected to blind docking analysis using BioLuminate interface (Schrödinger, LLC, New York, NY, 2020), as their binding regions were not known. Here, PIPER protein-protein docking algorithm was used that generated a cluster of structures based on parameters such as electrostatic, hydrophobic and Van der Waals interactions. These poses were further given to Prime MM-GBSA (Molecular mechanics using Generalized Born and Surface Area continuum) [8]docking for binding energy calculation (Prime, Schrödinger, LLC, New York, NY, 2020) and ranked accordingly based on cluster size, free energy (ΔG) and RMSD (Root Mean Squared Deviation) values. The top-ranked complexes were chosen for interaction analysis using PDBSum [9] followed by equilibration Molecular Dynamics (MD) simulation and metadynamics analysis.

2.3. MD simulation and metadynamics study of the docked complexes

To understand the stability of the HtrA2-cFLIP interacting region, molecular dynamics (MD) simulation was performed (Desmond, Schrödinger, LLC, New York, NY, 2020). The top three ranked HtrA2-cFLIP complexes were simulated for 200 ns to generate cluster of structures at 10ps intervals (detailed protocols in **Supplementary M4**). For each complex, 20000 structures were generated and accumulated in a cluster to assess the interacting H-bond, salt-bridges and van der Waal's interactions. The interacting residues identified by the PDBSum server (mentioned in the above method section) were assessed at each of these clusters, and the percentage survival index or PSI (percentage ratio between the total number of interactions survived for each residue in a cluster and total number of structures in the cluster) was calculated for the interacting residues. PSIs for residues from HtrA2 and cFLIP were separately tabulated for all three complexes and top 10 high PSIs were plotted.

Following PSI calculation, few of the high scoring HtrA2 residues were mutated to alanine in the rank1 complex and a mutant HtrA2-cFLIP complex was generated to predict the role the mutated residues in overall HtrA2-cFLIP interactions through metadynamic analysis (detailed protocols in **Supplementary M4**).

2.4. Purification of cFLIP DEDs and HtrA2 variants

The DEDs and HtrA2 variants [10] were purified using affinity chromatography as detailed in **Supplementary M5**.

2.5. Pull-down assays

Pull-down assay [11] was performed to check the interaction of full-length cFLIP with full-length inactive HtrA2 (S174A) and N-SPD as detailed in **Supplementary M6**.

2.6. Protease cleavage assay of cFLIP

Gel-based proteolytic assays [10,12] of full-length active HtrA2 with cFLIP and with DEDs as substrates were set up as mentioned in **Supplementary M7**.

2.7. Mass spectrometric analyses

For in-gel digestion sample preparation, an enzyme assay was set up for 8 h. After incubation, the cleaved fragment was excised from the silver-stained 15% tris-tricine gel [13]. The detailed protocol is mentioned in **Supplementary M8**.

3. Results

3.1. Purification of HtrA2 and cFLIP variants using affinity chromatography

The results of protein purification are shown in Fig. S1. The His_6 tagged proteins cFLIP DEDs (Fig. S1A), catalytically inactive HtrA2 (S174A) and active HtrA2 (Figs. S1B and S1C) were purified on Ni-NTA resin and eluted using a gradient of imidazole. The proteins of interest were eluted in the 250 mM imidazole fractions. N-SPD was purified using tandem purification first with MBP tag using amylose resin (Fig. S1D) followed by TEV cleavage to separate MBP and further purification using His_6 tag (Fig. S1E). The purity of the elutes as checked on SDS-PAGE showed that all the purified proteins were >95% pure and hence were further used for pull-downs and enzyme assays.

3.2. Biophysical studies show cFLIP to be stable with a well-folded secondary structure

Far UV CD spectropolarimetry of full-length cFLIP was performed to determine its secondary structural properties. The two dips in the spectra at 208 nm and 222 nm, commonly associated with the presence of alpha-helical structures (Fig. 1B) suggested that the protein possesses a significant amount of alpha-helical content that holds true since the tandem DEDs of cFLIP are hexa-helical structures. Thermal denaturation using CD as a function of temperature (20 °C–98 °C) was recorded that showed the protein to be stable. The melting temperature (T_m) determined after plotting and fitting the graph for temperature versus fraction unfolded was found to be 66 °C (Fig. 1C). The fluorescence emission scans of cFLIP (three tryptophan residues) were acquired after excitation at 295 nm. The excitation resulted in a 15 nm red shift for the urea-denatured protein (Fig. 1D). These studies suggested that the purified native cFLIP has an intact secondary structure and maintains a well-folded conformation, as demonstrated by the CD analysis and by

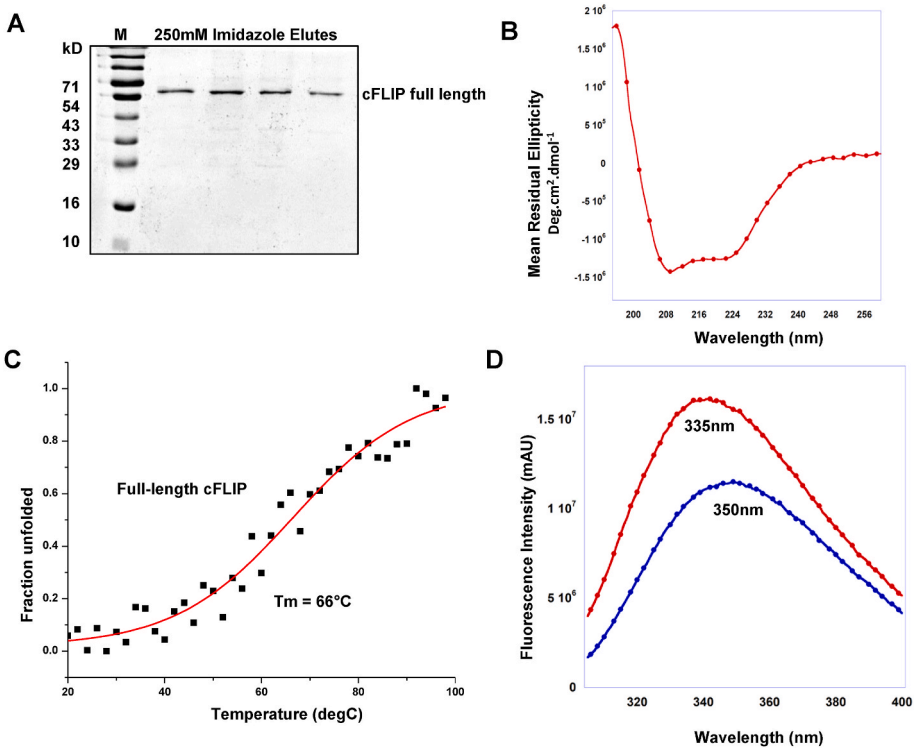

Fig. 1. Purification and biophysical characterization of full-length cFLIP- A) Full-length cFLIP protein was purified using Ni-NTA affinity chromatography and the 250 mM fractions were loaded on a 12% SDS-PAGE and visualized using Coomassie brilliant blue staining **B)** Far-UV CD spectra for purified and dialyzed cFLIP where scan was taken in the range from 198 nm to 260 nm. **C)** Thermal denaturation study of cFLIP within a temperature range of 20–98 °C. The data was normalized and plotted against temperature to obtain Tm **D)** Fluorescence emission spectra were recorded for native (red) and unfolded (blue) cFLIP, excited at 295 nm with emission between 310 nm and 400 nm. Emission maxima were observed at 335 nm (native) and 350 nm (unfolded) cFLIP. Experiments were performed in triplicates, and the averaged, normalized data was plotted. (For interpretation of the references to colour in this figure legend, the reader is referred to the Web version of this article.)

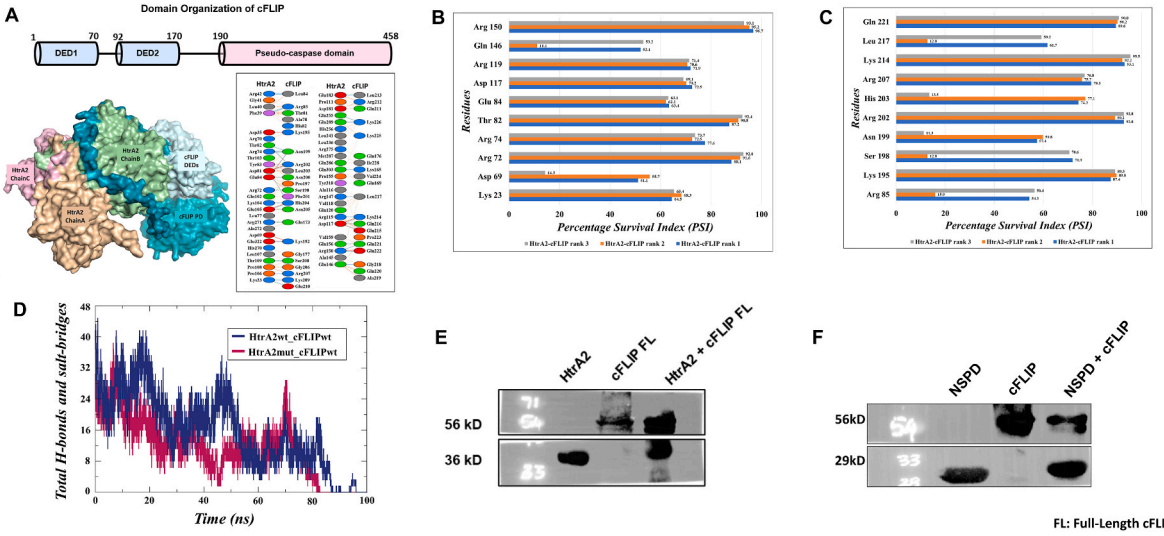

Fig. 2. In-silico and in-vitro studies to confirm cFLIP/HtrA2 interaction- A) Surface representation of the HtrA2-cFLIP complex, with HtrA2 chains A, B, and C in yellow, green, and pink, and cFLIP in cyan. The right panel illustrates the binding interface residues using PDBSum representation, with blue lines indicating hydrogen bonds, red lines representing salt bridges, and orange dashes indicating van der Waal's contacts. Bar plots representing the top 10 **(B)** HtrA2 residues and **(C)** cFLIP residues involved in formation of HtrA2-cFLIP complex where the PSI (Percentage Survival Index) values are given in X-axis and residue name in Y-axis. PSI values of rank1, rank2 and rank3 complexes are indicated as blue, orange, and grey bars, respectively. **D)** Graphical representation of metadynamics analysis showing the decline in H-bonds and salt-bridge count (Y-axis) over 100 ns (X-axis). Blue line - HtrA2-cFLIP wildtype complex, maroon line - mutant complex **E)** Pull-down assay between full-length (FL) cFLIP and HtrA2 confirming their interaction **F)** Pull-down assay between N-SPD of HtrA2 with full-length cFLIP showing interaction at the domain level. (For interpretation of the references to colour in this figure legend, the reader is referred to the Web version of this article.)

tryptophan fluorescence studies.

3.3. In-silico study predicts the predominant role of N-SPD region residues in HtrA2-cFLIP interaction

The domain organization of cFLIP with tandem DEDs and a pseudo-protease domain is shown in Fig. 2A. Molecular docking of the loop filled trimeric HtrA2 and the cFLIP AlphaFold structure resulted generation of a total of 19 different docked poses with RMSDs ranging from 1.07 Å to 4.30 Å; and cluster sizes from 315 to 7 **(Table S1)**. The poses were ranked according to their ΔG values, which were calculated for the lowest energy conformer in each cluster and ranged from −19.92 to −7.87 kcal/mol **(Table S1)**. The top three poses with ΔG values of −19.92, −19.01 and −17.02 kcal/mol were considered as their RMSDs ranged below 2 Å and would provide reliable prediction of the binding interfaces [14,15]. In all the three complexes, the interactions formed between HtrA2 and cFLIP majorly involved one subunit of the HtrA2 trimer, whereas other two subunits formed some residual interactions (Figs. S2–S4). In case of the rank1 complex, the HtrA2's chain B was involved in forming interaction with cFLIP (Fig. 2A and Fig. S1A), whereas, rank2 and rank3 complexes involved chain A (Fig. S3A) and chain C (Fig. S3A), respectively. Detailed analysis of the binding interface revealed that cumulative interactions involving H-bonds and salt bridges in rank1, rank2 and rank3 complexes were 43 (36 H-bonds and 7 salt bridges), 43 (38 H-bonds and 5 salt bridges) and 36 (30 H-bonds and 6 salt bridges) respectively (Figs. S2–S4). In the rank1 complex, out of 43, 38 H-bonds and salt-bridges involved N-SPD region residues of HtrA2 (Fig. S2B). A similar trend was also observed in other two complexes, where 34 out of 43 and 31 out of 36 interactions were formed by N-SPD region residues in rank2 and rank3 complexes, respectively (Figs. S3B and S4B). This dominant involvement of the N-SPD region residues in interaction with cFLIP was further supported by the MD simulation studies that analyzed a total of 60000 structures in three different clusters of the top three complexes in a timescale of 200 ns. MD analyses showed that all the top 10 longest surviving HtrA2 residues interactions were from the N-SPD region. They were namely, Lys23, Asp69, Arg72, Arg74, Thr2, Glu84, Asp117, Arg119, Gln146 and Arg150 (Fig. 2B). On the other hand, in cFLIP mostly the residues in the linker region between DED and protease domain formed interactions with HtrA2 (Figs. S2–S4), and after MD analyses, top 10 cFLIP counterpart residues were Arg85, Lys195, Ser198, Asn199, Arg202, His203, Arg207, Lys214, Leu217 and Gln221 (Fig. 2C).

Among the top 10 N-SPD region residues that were involved in HtrA2-cFLIP interactions, Arg72, Thr82 and Arg150 scored PSI >90 in at least two out of the three complexes (Fig. 2B). To understand the significance of these residues in HtrA2-cFLIP binding, they were mutated to alanine (as described in the method section) in rank1 complex and subjected to metadynamic study, where the wildtype rank1 complex was kept as control. In 100 ns metadynamic run, 0.03 kcal/mol of Gaussian height (GH) was exerted at periodic interval of 1 ps, which was equivalent to accumulated GH of 3000 kcal/mol. In both wildtype and mutant rank1 complexes, the binding interface residues residing in chain B of HtrA2 molecule and cFLIP molecule were targeted by the accumulated GH and the reduction of the H-bond and salt-bridge interactions were traced throughout 100 ns, finally resulting to HtrA2-cFLIP dissociation. It was observed that in case of the wildtype, total dissociation was culminated at 96.8 ns, which indicated an accumulation of ~2904 kcal/mol of GH for wildtype HtrA2-cFLIP dissociation (Fig. 2D). However, in case of the mutant, the complete dissociation occurs at 82.2 ns, thus requiring a total GH of ~2466 kcal/mol (Fig. 2D). Although, the mutation of three critical residues of HtrA2 did not completely disrupt the HtrA2-cFLIP interaction, there was a considerable reduction in GH or Gaussian energy, further implicating the role of Arg72, Thr82 and Arg150 residues. Involvement of these residues indicates the overall importance of N-SPD region in forming interactions with cFLIP and can be proven further using experimental validation.

3.4. In-vitro pull-down assay validates HtrA2-cFLIP interaction

Purified HtrA2 and its variants (Fig. S1) were used for pull-down assay and confirming the interaction with cFLIP. Pull-down assay followed by western blotting demonstrated that the full-length cFLIP and HtrA2 interact with each other as seen in Fig. 2E. Based on *in silico* leads indicating the importance of N-SPD, a pull-down assay with N-SPD showed that it interacts with cFLIP (Fig. 2F). These assays validate the results obtained through docking and MDS studies and establish the role of N-SPD being involved in interaction.

3.5. Gel based enzyme assay shows that active HtrA2 cleaves full-length cFLIP

Time-based proteolytic assays (between 0 min and 8 h) showed that HtrA2 cleaved full-length cFLIP within 2–3 h, demonstrating it as a substrate of HtrA2 as analyzed on SDS-PAGE in triplicates (Fig. 3A). A graph of time versus uncleaved full-length cFLIP was plotted as a function of time after normalizing the data considering cFLIP at 0 min (Fig. 3B). Similar studies with purified DEDs showed no cleavage (Fig. 3C) suggesting that the cleavage site(s) are not located in the DEDs. Furthermore, N-SPD alone was unable to cleave cFLIP thus reiterating the importance of the PDZ domains in regulating HtrA2 activity [4,10,16,17] (Fig. 3D). These studies confirmed that the C-terminal region of cFLIP is cleaved by full-length HtrA2.

3.6. Mass spectrometric analyses predict the site of cFLIP cleavage by HtrA2

An in-gel digestion was performed with the specific cleaved fragment (~32 kDa) of substrate identified through silver staining and subsequently subjected to mass spectrometric analysis. Fig. 4A highlights the identification of cFLIP protein and shows the generation of 11 peptides after trypsin digestion. The 11 cFLIP peptides obtained (shown in green in Fig. 4B) aligned with cFLIP DEDs validating cleavage occurs beyond DEDs. The cFLIP peptides were identified with >99% confidence and have been listed in Fig. 4C. The specificity of classical serine proteases is primarily determined by the positions of residues at the carboxyl-terminal (Prime - P1′, P2′, P3′) and amino-terminal (Nonprime - P1, P2, P3) relative to the cleavage site. These positions are stabilized by enzyme subsite residues (S3 to S3′) within the specificity pocket. Proteomic data shows HtrA2 selected charged amino acid (K) at the P1 position, aligning with other HtrA homologs. The P2 position features a polar amino acid (Q), P3 an aliphatic hydrophobic residue (V), and P4 an acidic residue (E). At P1′, there is a preference for an aromatic residue (F), while P2′ and P4′ are filled with aliphatic hydrophobic residue (L) and a basic side chain residue (H) at P3'. In summary, these observations are consistent with the enzyme assay studies, where the DEDs remain uncleaved by HtrA2.

4. Discussion

Aberrant apoptosis plays a role in various diseases like organ ischemia/reperfusion injury, diverse forms of cancers, and neurodegenerative/autoimmune disorders [18]. Serine protease HtrA2, involved in complex cellular processes and diverse diseases, is a promising therapeutic target linked to ischemic heart diseases, cancer, and neurodegenerative disorders [19,20]. This study aimed to investigate the interaction between proapoptotic HtrA2 and its antiapoptotic binding partner cFLIP, revealing their role in the apoptotic pathway and exploring the broad substrate preferences of this mammalian protease [11,12,21]. Limited research on HtrA2's substrate specificity through small peptide libraries [16] has created ambiguities in understanding its complex allosteric activation mechanism, constraining its utility in designing effective small molecule modulators. Therefore, to study HtrA2's substrate preferences and activation, exploring its interactions

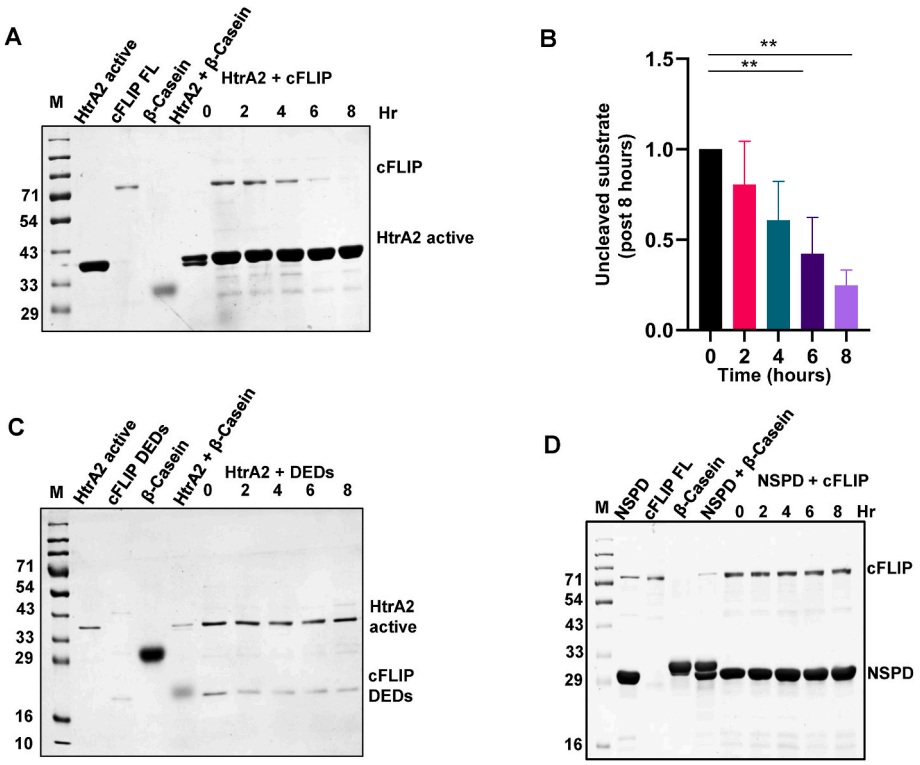

Fig. 3. Enzyme assay shows HtrA2 cleaves full-length cFLIP- A) Proteolytic activity of HtrA2 with full-length cFLIP **B)** Bar graph representing the amount of substrate left after 8 h relative to the uncleaved substrate. The error bars represent the standard errors (SE) calculated from three independent experiments ($p < 0.01$-**) **C)** Enzyme activity of HtrA2 with DEDs only **D)** Protease assay between trimeric N-SPD and full-length cFLIP. For all the enzyme assays, enzyme and substrate were incubated from 0 to 8 h at 37 °C and the samples were resolved on 12% SDS-PAGE gel and visualized using Coomassie Brilliant Blue staining. (For interpretation of the references to colour in this figure legend, the reader is referred to the Web version of this article.)

with natural cellular substrates becomes imperative [12,21]. Previous studies from our lab have identified novel substrates like GRIM19 and DUSP9 for this protease, revealing the broad specificity of HtrA2 at the cleavage site through N-terminal sequencing. Antiapoptotic cFLIP has been found to be overexpressed in several cancers and hence is a potential therapeutic target [22]. However, its structural similarity with procaspase-8 [23] limits research on the design of its specific inhibitor. Therefore, identifying another alternative approach to mitigate cFLIP function might provide an avenue toward effective drug design. HtrA2 influences the cell death pathways by cleaving anti-apoptotic proteins [24] through its serine protease activity. In this study, interdisciplinary approaches demonstrate the domain-level interaction between HtrA2 and the anti-apoptotic protein cFLIP, establishing the latter as a substrate of the protease. Biophysical characterization of purified full-length cFLIP exhibits stability and a properly folded tertiary structure. Molecular docking analyses highlight the crucial role of the N-SPD region in HtrA2 for its interaction with cFLIP. Comparative metadynamics offer insights into the HtrA2-cFLIP complex stability, revealing the putative minimal binding region. For cFLIP, interacting residues are in the linker between DEDs and the pseudo-protease domain. In HtrA2, the N-SPD is primarily involved in interaction. Enzyme assays revealed that HtrA2 cleaves full-length cFLIP, establishing it as a novel substrate for the protease. Notably, the trimeric active N-SPD (without PDZ) lacks the ability to cleave the substrate, emphasizing the crucial role of the PDZ domain in substrate catalysis and overall enzyme efficiency. Our previous data with GRIM19 [12] and XIAP [4] demonstrate the dispensability of the PDZ domain in this interaction and instead highlights that other regions play pivotal roles in facilitating the HtrA2-GRIM-19 interaction, illustrating the protease's adaptability in binding partners through different domains.

Our study reveals that HtrA2 does not cleave the DEDs, suggesting the cleavage site is located beyond them. This may be due to the tightly packed hexa-helical bundles within the DEDs, making them inaccessible to HtrA2 cleavage. Comparison of sequence specificities at different primary cleavage sites (P1–P4 and P1′-P4′) of cFLIP with peptide library studies [25] as well as with its natural substrate GRIM-19 show no preference for any subtype of amino acid *per se* [12]**(Table S2)**. For example, while P1 position accommodates a basic residue (K) in cFLIP, it is very well replaced by acidic, aliphatic, and polar residues in both peptidic substrates and GRIM-19. This observation reiterates the fact that HtrA2's substrate recognition is more complex than being just limited at the primary sequence level around the active site. Previous studies from our lab demonstrated the importance of initial substrate binding at the allosteric sites to be the key toward its recognition and specificity [2,26]. Unlike trypsin [27], which has specific peptide bond targets within a single protein, HtrA2 displays broad substrate specificity. This highlights its involvement in various cellular pathways and its exceptional adaptability to diverse binding mechanisms and partners across its domains.

In summary, this investigation holds significance as it unveils a novel substrate for HtrA2, offering valuable insights into the cellular substrate preferences of this enzyme. Understanding the interaction and intricate cleavage mechanisms of antiapoptotic proteins by cellular enzymes would lead to developing protein-protein interaction modulators, which would be instrumental in fine-tuning pathways for disease-specific therapeutic benefits.

Funding

This work is supported by (1) Grant (BT/HRD/NBA/May 37, 2015) awarded under the National Women Bio scientist Young Category by Department of Biotechnology (DBT), Govt. of India (2) Grant INT/RUS/RFBG/395 awarded by the Department of Science and Technology, International Bilateral Cooperation Division, Govt. of India, and (3)

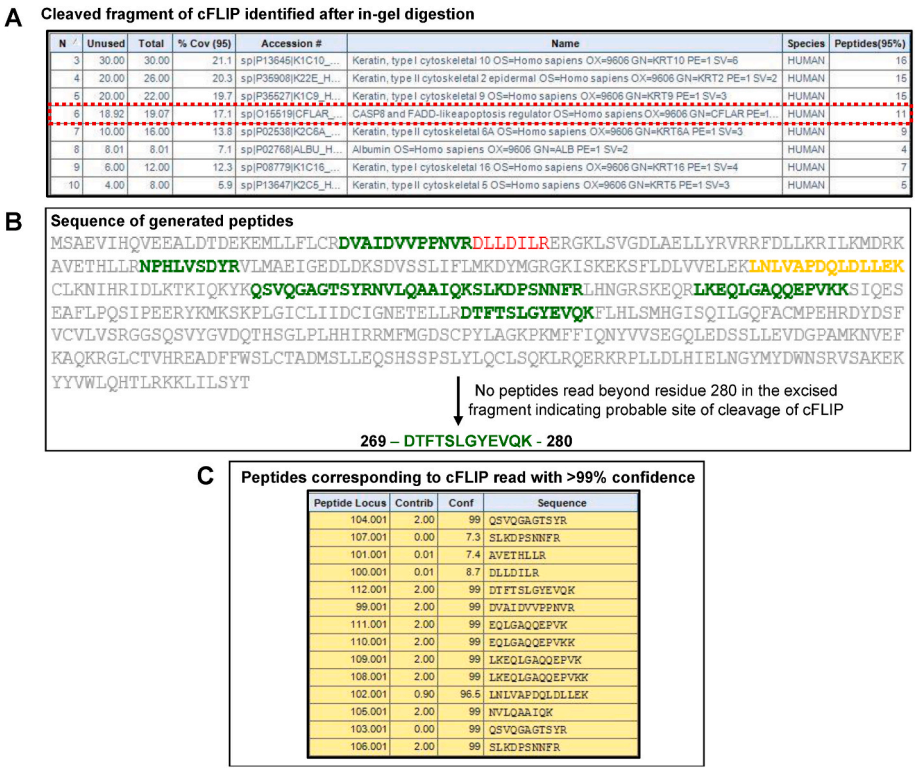

N	Unused	Total	% Cov (95)	Accession #	Name	Species	Peptides(95%)
3	30.00	30.00	21.1	sp|P13645|K1C10_...	Keratin, type I cytoskeletal 10 OS=Homo sapiens OX=9606 GN=KRT10 PE=1 SV=6	HUMAN	16
4	20.00	26.00	20.3	sp|P35908|K22E_H...	Keratin, type II cytoskeletal 2 epidermal OS=Homo sapiens OX=9606 GN=KRT2 PE=1 SV=2	HUMAN	15
5	20.00	22.00	19.7	sp|P35527|K1C9_H...	Keratin, type I cytoskeletal 9 OS=Homo sapiens OX=9606 GN=KRT9 PE=1 SV=3	HUMAN	15
6	18.92	19.07	17.1	sp|O15519|CFLAR_...	CASP8 and FADD-like apoptosis regulator OS=Homo sapiens OX=9606 GN=CFLAR PE=1...	HUMAN	11
7	10.00	16.00	13.8	sp|P02538|K2C6A_...	Keratin, type II cytoskeletal 6A OS=Homo sapiens OX=9606 GN=KRT6A PE=1 SV=3	HUMAN	9
8	8.01	8.01	7.1	sp|P02768|ALBU_H...	Albumin OS=Homo sapiens OX=9606 GN=ALB PE=1 SV=2	HUMAN	4
9	6.00	12.00	12.3	sp|P08779|K1C16_...	Keratin, type I cytoskeletal 16 OS=Homo sapiens OX=9606 GN=KRT16 PE=1 SV=4	HUMAN	7
10	4.00	8.00	5.9	sp|P13647|K2C5_H...	Keratin, type II cytoskeletal 5 OS=Homo sapiens OX=9606 GN=KRT5 PE=1 SV=3	HUMAN	5

Peptide Locus	Contrib	Conf	Sequence
104.001	2.00	99	QSVQGAGTSYR
107.001	0.00	7.3	SLKDPSNNFR
101.001	0.01	7.4	AVETHLLR
100.001	0.01	8.7	DLLDILR
112.001	2.00	99	DTFTSLGYEVQK
99.001	2.00	99	DVAIDVVPPNVR
111.001	2.00	99	EQLGAQQEPVK
110.001	2.00	99	EQLGAQQEPVKK
109.001	2.00	99	LKEQLGAQQEPVK
108.001	2.00	99	LKEQLGAQQEPVKK
102.001	0.90	96.5	LNLVAPDQLDLLEK
105.001	2.00	99	NVLQAAIQK
103.001	0.00	99	QSVQGAGTSYR
106.001	2.00	99	SLKDPSNNFR

Fig. 4. Mass spectrometric study delineates the cleavage site of cFLIP- A) list of the proteins identified after mass spectrometry **B)** peptides generated (shown in green) by in-gel digestion of the cleaved fragment from the substrate cFLIP resolved on a 15% tris-tricine gel followed by silver staining and **C)** list showing the peptides corresponding to cFLIP identified with >99% confidence. (For interpretation of the references to colour in this figure legend, the reader is referred to the Web version of this article.)

TRAC/0416/900198/001 IEC Project No. 198 funded by ACTREC-TMC.

Data availability statement

The data is available with the corresponding author and can be made available upon request.

CRediT authorship contribution statement

Kalyani Natu: Writing – review & editing, Writing – original draft, Visualization, Validation, Software, Methodology, Investigation, Formal analysis, Conceptualization. **Shubhankar Dutta:** Writing – review & editing, Writing – original draft, Visualization, Software, Methodology, Investigation, Formal analysis. **Kakoli Bose:** Writing – review & editing, Supervision, Resources, Project administration, Conceptualization.

Declaration of competing interest

The authors declare that they have no known competing financial interests or personal relationships that could have appeared to influence the work reported in this paper.

Acknowledgements

The authors thank Biophysics Facility and Mass Spectrometry Facility, ACTREC for providing infrastructure for the necessary experiments.

Appendix A. Supplementary data

Supplementary data to this article can be found online at https://doi.org/10.1016/j.bbrep.2024.101682 View High-Res Image.

References

[1] L.C. Gavrilescu, E.Y. Denkers, Apoptosis and the balance of homeostatic and pathologic responses to Protozoan infection, Infect. Immun. 71 (2003) 6109–6115.
[2] A.L. Parui, et al., Inter-subunit crosstalk via PDZ synergistically governs allosteric activation of proapoptotic HtrA2, Structure 30 (2022) 1307–1320.e5.
[3] A. Chakraborty, R. Bose, K. Bose, Unraveling the dichotomy of enigmatic serine protease HtrA2, Front. Mol. Biosci. 9 (2022).
[4] A.L. Parui, N. Singh, S. Dutta, K. Bose, Role of conserved regulatory loop residues in allosteric propagation of serine protease HtrA2, Biochem. Biophys. Res. Commun. 594 (2022) 63–68.
[5] Y. Suzuki, et al., Mitochondrial protease Omi/HtrA2 enhances caspase activation through multiple pathways, Cell Death Differ. 11 (2004) 208–216.
[6] J.S. Riley, et al., DED or alive: assembly and regulation of the death effector domain complexes, Cell Death Dis. 6 (2015) e1866.
[7] M. Merski, Molecular motion regulates the activity of the mitochondrial serine protease HtrA2, Cell Death Dis. 8 (2017) e3119–e3119.
[8] T. Hou, et al., Assessing the performance of the molecular mechanics/Poisson Boltzmann surface area and molecular mechanics/generalized Born surface area methods. II. The accuracy of ranking poses generated from docking, J. Comput. Chem. 32 (2011) 866–877.
[9] R.A. Laskowski, et al., PDBsum: structural summaries of PDB entries, Protein Sci. 27 (2018) 129–134.
[10] L.K. Chaganti, et al., Intricate structural coordination and domain plasticity regulate activity of serine protease HtrA2, Faseb. J. 27 (2013) 3054–3066.
[11] L.K. Chaganti, et al., Structural modeling and role of HAX-1 as a positive allosteric modulator of human serine protease HtrA2, Biochem. J. 476 (2019) 2965–2980.
[12] R. Kummari, et al., Elucidating the role of GRIM-19 as a substrate and allosteric activator of pro-apoptotic serine protease HtrA2, Biochem. J. 478 (2021) 1241–1259.
[13] A. Shevchenko, et al., Mass spectrometric sequencing of proteins from silver-stained polyacrylamide gels, Anal. Chem. 68 (1996) 850–858.
[14] D. Ramírez, J. Caballero, Is it reliable to take the molecular docking top scoring position as the best solution without considering available structural data? Molecules 23 (2018) 1038.
[15] K.E. Hevener, Validation of molecular docking programs for virtual screening against dihydropteroate synthase, J. Chem. Inf. Model. 49 (2009) 444–460.
[16] P.R. Bejugam, et al., Allosteric regulation of serine protease HtrA2 through novel non-canonical substrate binding pocket, PLoS One 8 (2013) e55416.
[17] N. Singh, et al., Dual regulatory switch confers tighter control on HtrA2 proteolytic activity, FEBS J. 281 (2014) 2456–2470.

[18] M.S. Bhuiyan, K. Fukunaga, Activation of HtrA2, a mitochondrial serine protease mediates apoptosis: current knowledge on HtrA2 mediated myocardial ischemia/reperfusion injury, Cardiovascular Therapeutics (2008) 26 224–232, https://doi.org/10.1111/j.1755-5922.2008.00052.x. Preprint at.
[19] M.S. Bhuiyan, K. Fukunaga, Mitochondrial serine protease HtrA2/omi as a potential therapeutic target, Curr. Drug Targets 10 (2009).
[20] M.S. Bhuiyan, K. Fukunaga, Inhibition of HtrA2/Omi ameliorates heart dysfunction following ischemia/reperfusion injury in rat heart in vivo, Eur. J. Pharmacol. 557 (2007) 168–177.
[21] S. Acharya, et al., Dual specificity phosphatase 9: a novel binding partner cum substrate of proapoptotic serine protease HtrA2, Biochem. Biophys. Res. Commun. 533 (2020) 607–612.
[22] M. Bagnoli, et al., Cellular FLICE-inhibitory protein (c-FLIP) signalling: a key regulator of receptor-mediated apoptosis in physiologic context and in cancer, Int. J. Biochem. Cell Biol. 42 (2010) 210–213.
[23] M.A. Hughes, et al., Co-Operative and hierarchical binding of c-FLIP and caspase-8: a unified model defines how c-FLIP isoforms differentially control cell fate, Mol. Cell 61 (2016) 834–849.
[24] A.M. Verhagen, et al., HtrA2 promotes cell death through its serine protease activity and its ability to antagonize inhibitor of apoptosis proteins, J. Biol. Chem. 277 (2002) 445–454.
[25] L.M. Martins, et al., Binding specificity and regulation of the serine protease and PDZ domains of HtrA2/Omi, J. Biol. Chem. 278 (2003) 49417–49427.
[26] N. Singh, et al., Dual regulatory switch confers tighter control on HtrA2 proteolytic activity, FEBS J. 281 (2014) 2456–2470.
[27] W. Ma, et al., Specificity of trypsin and chymotrypsin: loop-motion-controlled dynamic correlation as a determinant, Biophys. J. 89 (2005) 1183–1193.